

Turbulence Measurements at High Reynolds Numbers Using a New Inclined Nano-Scale Thermal Anemometry Probe

M. Vallikivi, M. Hultmark and A. J. Smits

Department of Mechanical and Aerospace Engineering
 Princeton University, New Jersey, USA

Abstract

The first efforts towards building and testing a multicomponent Nano-Scale Thermal Anemometry Probe (NSTAP) are reported for studies of high Reynolds number turbulence. An inclined NSTAP has been fabricated and tested in a turbulent pipe flow over a range of Reynolds numbers and it is shown to be in good agreement with available data. Specifically, the results demonstrate the feasibility of implementing the inclined NSTAP design in wall-bounded turbulence at high Reynolds number.

Introduction

Hot-wires continue to be the method of choice for turbulence measurements, primarily because they yield time-resolved data with relatively good temporal and spatial resolution. With increasing Reynolds number, however, the finite size of the wires limits the range of scales that can be fully resolved [1, 2, 3, 4]. In order to overcome these limitations, we have developed a novel thermal anemometer that has an order of magnitude smaller wire filament and can therefore be used in much higher Reynolds number flows than conventional probes. Fabrication of these new devices, namely Nano-Scale Thermal Anemometry Probes (NSTAPs), involves semiconductor and micro-electro-mechanical system (MEMS) fabrication techniques that have been thoroughly described elsewhere [5].

These new nanoscale probes are operated similarly to conventional hot wire probes, and the results have been compared to those obtained using hot wires in a number of different flows (see [5, 6]). The results demonstrated excellent agreement between NSTAP and hot wire data in the Reynolds number regime where both are expected to give identical results. In addition, NSTAPs have been used at much higher Reynolds numbers where their superior temporal and spatial resolution become essential (see [7, 8]).

These measurements were performed using single NSTAP sensors with the wire oriented normal to the flow (hereafter 'normal wires')¹. However, normal wires give only one component of velocity, that is, the streamwise component $u = \bar{u} + u'$. Here the overbar denotes a time average, and the prime denotes the fluctuating component. In wall-bounded turbulent flows the principal phenomenon of interest is the wall-normal transport, and therefore the wall-normal component, v' , and the Reynolds shear stress, $-\overline{u'v'}$, are the more important quantities. To measure the wall-normal component, cross-wire anemometry probes are commonly used, but building a cross-wire probe using MEMS fabrication techniques is extremely challenging. Here we take the first step in that direction by manufacturing and testing NSTAP probes with a single inclined sensing element to demonstrate that the NSTAP concept is suitable for multicomponent velocity measurements, and present the preliminary results in a pipe flow with $75 \times 10^3 \leq Re_D \leq 10^6$.

¹Although the sensor in the NSTAP is actually a flat ribbon $2\mu\text{m}$ wide, 100 nm thick, and either 60 or $30\mu\text{m}$ long, in this text we will call them "wires" to facilitate comparison with hot wire probes.

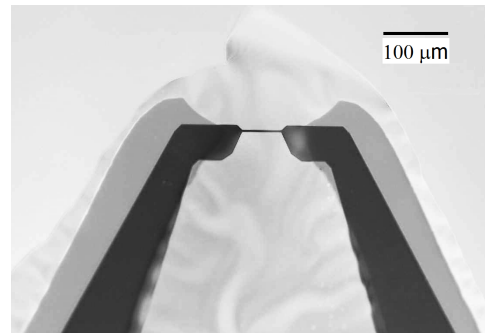


Figure 1: Image of a typical $60\mu\text{m}$ normal NSTAP probe. The black surfaces are the metal contacts, and the grey surfaces are the silicon supports.

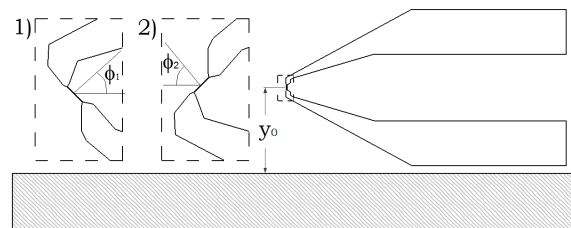


Figure 2: Layout of the sensor: 1) configuration inclined towards the wall, 2) inclined away from the wall. All dimensions given in microns.

Inclined Sensor

A typical $60\mu\text{m}$ normal wire NSTAP probe is shown in figure 1. In figure 2, a layout of the metal structure of the inclined NSTAP probe is shown together with the positioning of the sensor with respect to the wall, where y_0 is wall normal starting distance. Several inclined NSTAPs were fabricated using the techniques described in [5], and a typical $60\mu\text{m}$ probe is shown in figure 3. The grey areas in the background are the silicon supports. By comparing this image with that in figure 1, it can be seen that the supports for the normal wire probe are much "cleaner" and more streamlined than for the preliminary inclined wire design. It will take considerable additional work to optimize the support geometry, and so for our current purposes we proceed with probe shown in figure 3. The probe was mounted onto conventional hot-wire prongs for support, and a Dantec Streamline Constant Temperature Anemometry system with 1:1 bridge was used to operate the sensor.

Experiments

The experimental setup in this study was the same as that described in [7]. The experiments were conducted in the Princeton ONR Superpipe, a turbulent pipe flow facility capable of producing a very large Reynolds number range. These Reynolds numbers are achieved by varying the air pressure p in the pipe (with diameter $D = 129.4\text{ mm}$), as well as by changing

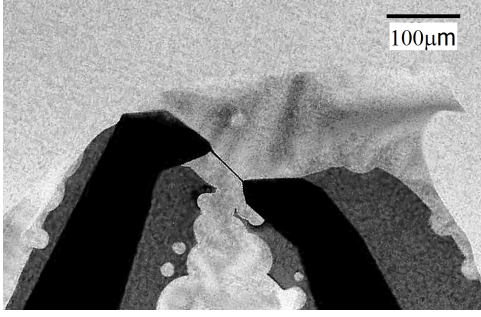


Figure 3: Image of a typical 60 μm inclined NSTAP probe. The black surfaces are the metal contacts, and the grey surfaces are the silicon supports.

the bulk velocity $\langle U \rangle$. Four Reynolds numbers were considered: $Re_D = \langle U \rangle D/\nu = 75 \times 10^3$, 165×10^3 , 458×10^3 , and 977×10^3 , with $\langle U \rangle = 8.8, 19.5, 10.4$, and 22.2 m/s, and $p = 1, 1, 5.2, 5.2$ atm, respectively. For further details, see [10].

To use a single inclined probe for measuring wall-normal fluctuations, two consecutive profiles need to be measured. In the first profile, the sensor is positioned in the flow at ϕ_1 to the mean flow, and in the second profile the sensor is rotated 180°, so the wire is positioned in the flow at an angle ϕ_2 to the mean flow (see figure 2). The crossflow sensitivity is assumed to be given by an effective cooling velocity $U_e = \mathbf{n} \cdot \mathbf{V}$, where \mathbf{V} is the velocity vector and \mathbf{n} is the unit vector normal to the wire. The cooling velocities U_{e1} and U_{e2} are then related to the stream-wise and wall-normal velocities by

$$U_{e1} = (\bar{u} + u') \cos \phi_1 + (\bar{v} + v') \sin \phi_1 \quad (1)$$

$$U_{e2} = (\bar{u} + u') \cos \phi_2 - (\bar{v} + v') \sin \phi_2 \quad (2)$$

where the subscripts 1 and 2 refer to the two different probe orientations as shown in figure 2. If the same probe is used for measuring both profiles it follows that $\phi_2 = \phi_1 = \phi$. Equations (1) and (2) can be rewritten as

$$f_i(E_i, \phi_i) = \frac{U_{ei}}{\cos \phi_i} = (\bar{u} + u') \pm (\bar{v} + v') \tan \phi_i \quad (3)$$

where $i = 1, 2$ denote the two probe orientations and E_i is the respective voltage output of the anemometer. By assuming that ϕ for a specific probe is a function of E only, the relationship $f = f(E)$ can be determined through a conventional velocity calibration. As in [11], we use fourth-order polynomials, so that

$$f_i = A_{0i} + A_{1i}\bar{E}_i + A_{2i}\bar{E}_i^2 + A_{3i}\bar{E}_i^3 + A_{4i}\bar{E}_i^4 \quad (4)$$

where A_{ji} are calibration constants determined by the velocity calibration. Velocity calibrations were performed at the centerline of the pipe using measurements from a Pitot probe as a reference. For each case, 14 points were acquired before and after every profile.

As a second step, the effective cooling angle needs to be found. For cross-wires, an in-situ calibration method suitable for fully-developed pipe flow was described by Zhao [11]. This method can also be used for single inclined wires, as seen below. In addition, we can adapt the calibration procedure proposed by Bradshaw [12], where the probe is tilted through a range of angles α and it was assumed that the effective cooling angle is changed by the same amount (see also [13]. This assumption yields

$$\frac{\bar{f}}{\bar{u}} = \sin \alpha \tan \phi + \cos \alpha \quad (5)$$

Therefore ϕ can be determined by fitting a straight line to the plot of \bar{f}/\bar{u} versus α .

The angle calibration was performed in a low speed wind tunnel by tilting the probe between $-15 < \alpha < 15$. For the probe used in this work, we found $\phi_{cal} = 31^\circ$ as determined by a linear fit to the data (see figure 4). This calibration was performed in laminar flow at $U = 30$ m/s and at atmospheric pressure. Angle calibrations at higher pressures were not possible in the current setup, although one might expect a slight change in the effective cooling angle with changing Reynolds number. The geometric angle made by the sensor to the probe axis was very close to 45° (see figure 3), 14° less than the value found by the angle calibration. The possibility of some aerodynamic interference due to the support structure in the current configuration cannot be ruled out.

Once the effective cooling angle ϕ is known, the variances $\overline{u'^2}$ and $\overline{v'^2}$ may be found using equations (3) as follows

$$\bar{u} = \frac{\bar{f}_1 + \bar{f}_2}{2} \quad (6)$$

$$\bar{v} = \frac{\bar{f}_1 - \bar{f}_2}{2 \tan \phi} \approx 0 \quad (7)$$

$$-\overline{u'v'} = \frac{\bar{f}_2'^2 - \bar{f}_1'^2}{4 \tan \phi} \quad (8)$$

$$\overline{u'^2} + \overline{v'^2} \tan^2 \phi = \frac{\bar{f}_1'^2 + \bar{f}_2'^2}{2} \quad (9)$$

where $-\overline{u'v'}$ can be compared with the distribution of the total stress τ_T in turbulent flow, which is given by

$$\tau_T = - \left(\frac{1}{2} \frac{dp}{dx} \right) (R - y) \quad (10)$$

where dp/dx is the pressure gradient, $R = D/2$ is the pipe radius, and y is the wall-normal distance. For $y^+ = yu_\tau/\nu > 250$

$$\tau_T \approx -\rho \overline{u'v'} \quad (11)$$

where ρ is the fluid density and u_τ is the friction velocity. The pressure gradient was measured directly using an array of static pressure tabs in the pipe wall. This provides us another method for determining the effective cooling angle ϕ , by fitting the results obtained for $-\overline{u'v'}$ using equation 8 and the known stress distribution given by equations 10 and 11 for $y^+ > 250$. This is the method first proposed by Zhao [11]. Compared to the angle calibration method expressed by equation 5, this fitting gives an opportunity to estimate a different ϕ for every studied Reynolds number. Using least square linear fit, the effective angle is found to be $\phi_{fit} = [26^\circ, 32^\circ, 31^\circ, 31^\circ]$ for respective Reynolds numbers $Re = [75 \times 10^3, 165 \times 10^3, 458 \times 10^3, 997 \times 10^3]$. The angles found for the higher Reynolds numbers are very close to that found from the Bradshaw calibration, $\phi_{cal} = 31$, which is encouraging.

Once the angle ϕ is known, \bar{u} , \bar{v} and $-\overline{u'v'}$ can be evaluated using equations 6, 7 and 8. To find $\overline{v'^2}$ some more information is needed, so normal wire measurements of $\overline{u'^2}$ at similar Reynolds numbers from [8] are used to find $\overline{v'^2}$ from equation 9.

To examine the effect of small changes in ϕ on the inferred turbulence stresses, the data were first processed using the effective cooling angle ϕ_{fit} determined from the $\overline{u'v'}$ distribution. Secondly, the cooling angle determined by the angle calibration was used, which gave $\phi_{cal} = 31^\circ$. The data were analyzed using both cooling angles, as discussed below.

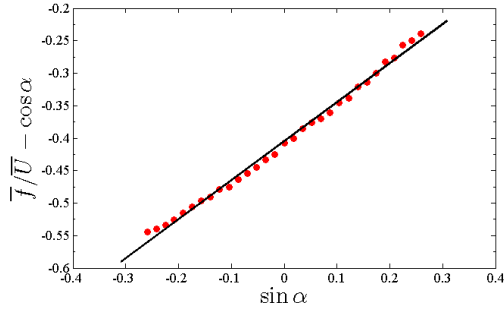


Figure 4: Angle calibration. Circles denote experimental data, and the line represents a linear fit with a slope $\tan \phi$.

Results

The streamwise mean velocity profiles obtained using the inclined wire NSTAP are shown in figure 5 in inner coordinates, that is, scaled with u_τ and ν . The data may be compared with the results from the single normal NSTAP measurements reported in [7] and [8], marked using open symbols in all graphs. It can be seen that the agreement between normal and inclined sensor mean velocities is very good (average variations about 4%). Note that the streamwise mean velocity profiles can be found without requiring the use of the effective cooling angle, and so the good agreement between datasets is not surprising. From figure 5 it can also be seen that the $\bar{v} \approx 0$ as expected in a pipe flow.

In figure 6, turbulent shear stress component $-\overline{u'v'^+}$ obtained from equation 8 is shown, compared to the shear stress found from the pressure gradient measurements in outer coordinates. The data is shown for $y^+ > 250$, the region where the distribution of $-\overline{u'v'^+}$ is expected to be linear. The cooling angle from the angle calibration was used to process the data. It may be seen that for the three higher Reynolds numbers the inclined NSTAP probe gives very satisfactory results for the Reynolds stress.

The radial turbulence intensities $\overline{v'^2}^+$ obtained from equation 9 are shown in figures 7 and 8, with the two different estimates for the cooling angle. The results were obtained using the measurements of u'^2^+ by Hultmark et al. [8], as required by equation 9. It is apparent that different cooling angle estimates give slightly different results, but the overall trends are very similar, with $\overline{v'^2}^+$ collapsing to some extent in the outer region and approaching a constant value near the wall. When the cooling angle ϕ_{fit} is used, as in figure 7, the Reynolds number trend is more noticeable and this could indicate that this is a better cooling angle estimate than the one given by ϕ_{cal} . The results are consistent with the expectation that all turbulent stresses should be of the same order at the pipe centerline, but the agreement between the different profiles near the wall is disappointing, since we would expect the wall-normal intensities to collapse at about the same plateau level (similar in value to that found by [14], also shown in the figures), regardless of the Reynolds number. This could be an effect of a poor estimate of the cooling angle, or uncertainties in determining the wall-normal distance, or it may simply be a result of the uncertainties involved in finding the difference between two large numbers.

Conclusions

The first inclined NSTAP has been fabricated and tested in turbulent pipe flow. The probe was used to make measurements of the shear stress and radial turbulence intensities in fully de-

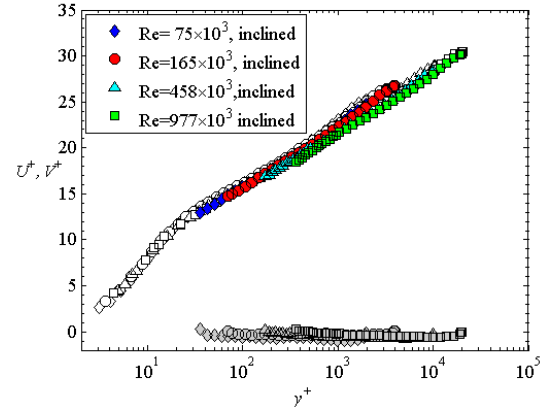


Figure 5: Mean velocities in inner variables. Streamwise velocity component: Open symbols denote normal NSTAP measurements from [7], colored symbols denote inclined wire measurements. Wall normal velocity component: grey symbols denote inclined wire measurements.

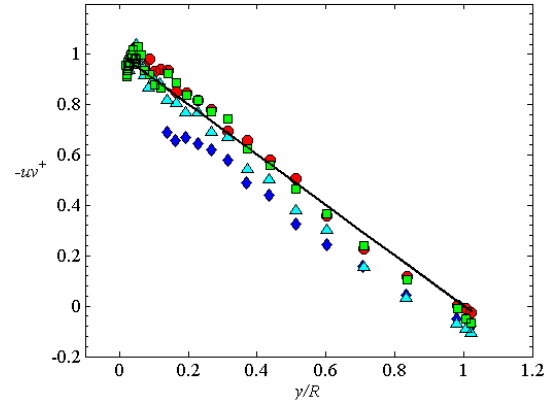


Figure 6: $-\overline{u'v'^+}$ in outer variables for $y^+ > 250$. Solid line represents $-\overline{uv}^+$ based on pressure gradient measurement. All other symbols are according to legend in figure 5.

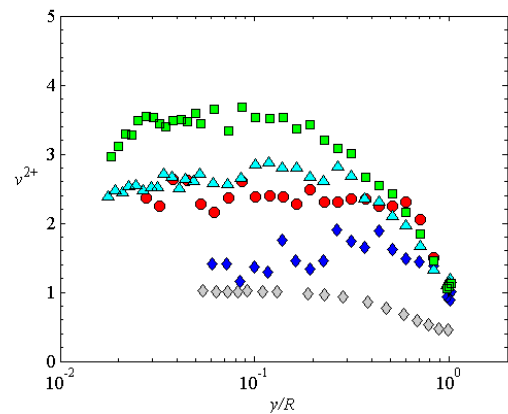


Figure 7: Wall-normal turbulence intensities in outer variables, using ϕ_{fit} . Grey diamonds indicate available data at $Re_D = 74 \times 10^3$ from [11]. All other symbols are according to legend in figure 5.

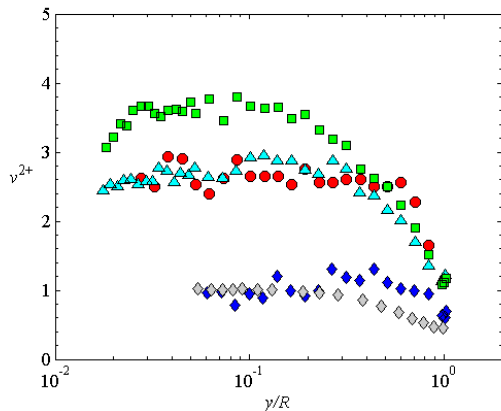


Figure 8: Wall-normal turbulence intensities in outer variables, using ϕ_{cal} . Grey diamonds indicate available data at $Re_D = 74 \times 10^3$ from [11]. All other symbols are according to legend in figure 5.

veloped pipe flow at Reynolds numbers between 75×10^3 and 10^6 . The results on the shear stress are encouraging, but the radial turbulence intensity shows considerable scatter. It is evident that great care has to be taken determining the angular response of the sensors. With further development of the probe, especially in reducing the possible aerodynamic interference on the sensor by using an improved geometry, better fabrication techniques, and more advanced calibration methods, it appears possible to use inclined NSTAPs for two component turbulence measurements, and to ultimately develop a multicomponent nano-scale sensor.

This work was made possible by support received through ONR Grant N00014-09-1-0263, program manager Ronald Joslin and NSF Grant CBET1064257, program manager Henning Winter.

References

- [1] Willmarth, W. W. and Sharma L. K., Study of turbulent structure with hot wires smaller than the viscous length *J. Fluid Mech.*, **142**, 121–149, 1984
- [2] Ligrani P. M. and Bradshaw P., Subminiature hot-wire sensors: development and use *J. Phys. E: Sci. Instrum.*, **20**, 323–332, 1987
- [3] Ligrani P. M. and Bradshaw P., Spatial resolution and measurement of turbulence in the viscous sublayer using subminiature hot-wire probes *Exp. in Fluids*, **6**, 407–417, 1987
- [4] Smits, A. J., Monty, J. P., Hultmark, M., Bailey, S. C. C., Hutchins, N. and Marusic, I. Spatial resolution correction for turbulence measurements, *J. Fluid Mech.*, **676**, 41–53, 2011.
- [5] Vallikivi, M., Hultmark, M., Bailey, S. C. C. and Smits, A. J. Turbulence measurements in pipe flow using a nano-scale thermal anemometry probe, *Exp. in Fluids*, **51**, 1521–1527, 2011.
- [6] Bailey, S. C. C., Kunkel, G. J., Hultmark, M., Vallikivi, M., Hill, J. P., Meyer, K. A., Tsay, C., Arnold, C. B. and Smits, A. J. Turbulence measurements using a nanoscale thermal anemometry probe, *J. Fluid Mech.*, **663**, 160–179, 2010.
- [7] Hultmark, M., Vallikivi, M., Bailey, S. C. C. and Smits, A. J. Turbulence at extreme Reynolds numbers, *Phys. Rev. Lett.*, **108**, doi: 10.1103/PhysRevLett.108.094501, 2012.
- [8] Hultmark, M., Vallikivi, M. and Smits, A. J. Logarithmic scaling of turbulence in smooth and rough-wall pipe flow at extreme Reynolds number, *J. Fluid Mech.*, under review, 2012.
- [9] Townsend, A. A. *The Structure of Turbulent Shear Flow*. 2nd ed., Cambridge University Press, 1976.
- [10] Zagarola, M. V. & Smits, A. J. Mean-flow scaling of turbulent pipe flow. *J. Fluid Mech.* **373**, 33–79, 1998.
- [11] Zhao, R., Li, J. and Smits, A. J. A new calibration method for crossed hot wires, *Meas. Sci. Technol.*, **15**, 1926–1931, 2004.
- [12] Bradshaw, P. B. *An Introduction to Turbulence and its Measurement*, Pergamon Press, 1971.
- [13] Jiménez, J., Hultmark, M., and Smits, A. J. The intermediate wake of a body of revolution at high Reynolds numbers. *J. Fluid Mech.* **659**, pp. 516–539, 2010.
- [14] Perry, A. E., Henbest, S. and Chong, M. S. A theoretical and experimental study of wall turbulence. *J. Fluid Mech.* **165**, pp. 163–199, 1986.